New Results from the H1 Collaboration

André Schöning *

University of Zurich - Department of Physics
Winterthurerstr. 190, CH-8057 Zürich - Switzerland
and
DESY
Notkestr. 85, D-22607 Hamburg - Germany

After more than 15 years, the operation of the world's unique electron-proton collider HERA ended in June 2007. The data collected by the H1 experiment correspond to a total integrated luminosity of about 0.5 fb^{-1}. In 2007 dedicated runs were taken at lower proton beam energies to measure the longitudinal proton structure function F_L. In this talk new results, many of them exploiting data taken after the HERA upgrade in the year 2000, and the first measurement of F_L are presented.

1 Introduction

After more than 15 years of successful data taking at HERA the H1 collaboration has started to finalise the data analyses and is entering a new era of high precision studies of the proton structure. The basis are the high quality data taken by the H1 experiment in electron- or positron-proton collisions at HERA I (year 2000 and before) and at HERA II (2003-2007) with a total integrated luminosity of about 0.5 fb^{-1}. At the upgraded HERA II longitudinally polarised electron or positron beams were provided regularly with polarisation degrees of 40% and more. The data were collected at center of mass energies of about 320 GeV (300 GeV before 1999) and 225 (275) GeV in dedicated runs with lowered proton beam energies of $E_p = 460$ (575) GeV in order to perform a first direct measurement of the longitudinal proton structure function F_L.

The main topics covered by this talk are deep inelastic scattering at high Q^2, tests of electroweak physics, searches beyond the Standard Model (SM), the study of the proton structure, jet physics, the measurement of the strong coupling and the study of exclusive final states like charm production.

2 Electroweak Physics and High Q^2

Using the full statistics of high energy HERA data the single differential neutral current (NC) cross section in deep inelastic scattering (DIS) is measured as function of the negative four momentum transfer squared Q^2. The cross sections are shown in Fig. 1 for e^+p and e^-p collisions separately. The cross sections, measured over a large Q^2 range, change by more than six orders of magnitude and are well described by the SM prediction based on the proton density function (PDF) previously published by H1 using only the HERA I data [6]. For $Q^2 \lesssim 1000$ GeV^2 the DIS interaction is dominated by photon exchange and the cross section scales like $1/Q^4$. For larger values of Q^2 the Z exchange and the $\gamma - Z$ interference contribute, the latter being responsible for the different cross sections between e^+p and e^-p at high Q^2.

*On behalf of the H1 collaboration.

3 Searches

The existence of new particles or new interactions of fermions or bosons would manifest as deviations from the SM expectations at high Q^2. These deviations can be described in the context of contact interactions if the mass of the new particles is much higher than the available energy of the studied reactions. Deviations from the SM are also expected in composite models if quarks or leptons have a finite size. Using the full HERA I+II data quark radii larger than $0.74 \cdot 10^{-18}$ m can be excluded.

New particles like leptoquarks (LQ), which are predicted by Grand Unified Theories, might have masses as light as the electroweak energy scale and could be resonantly produced at colliders. A search for first generation LQs (coupling to first generation leptons) has been performed by H1 using the full HERA data set. No significant deviation from the SM expectation is found and limits on the Yukawa coupling λ as function of the LQ mass are set. The exclusion regions for the $S_{0,L}$ type LQ, which corresponds also to the scalar d-quark in supersymmetric models, are shown in Fig. 2 and compared with results from other collider experiments. Similar results are also obtained in a search for LQs coupling to the first and second lepton generation.

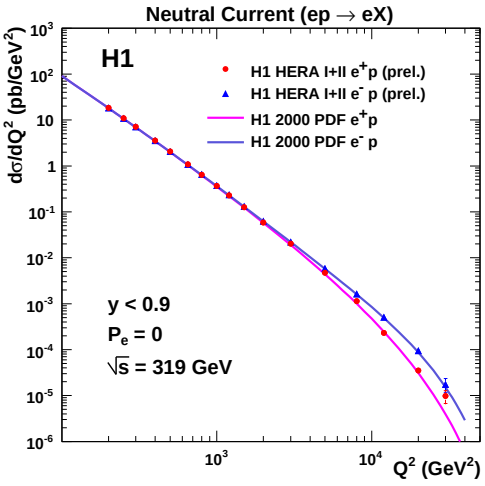

Figure 1: Single differential cross section $d\sigma/dQ^2$ for e^-p and e^+p as function of Q^2.

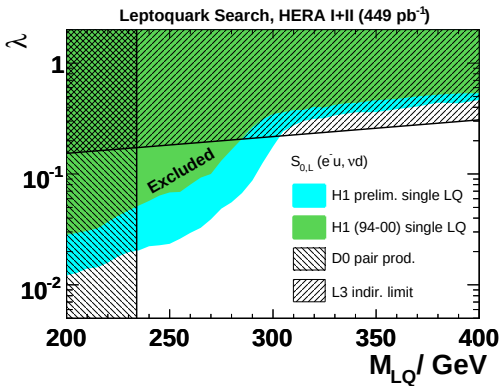

Figure 2: Exclusion limits at 95% CL on the coupling λ as a function of the leptoquark mass for $S_{0,L}$ using the HERA I+II data. The indirect limits of LEP (L3 and OPAL) and the direct limit from Tevatron (D0) are shown for comparison. The published H1 limit from HERA I is also shown.

In addition to the previous model dependent searches interesting final state topologies are investigated to search for possible deviations from the SM expectation. Of special interest are final states with leptons because of their clear signature and low background. In Fig. 3 (left) the scalar sum of the transverse momentum, $\sum P_T$, of final states containing two or three clearly identified high P_T electrons is shown using all HERA data from H1 and ZEUS combined corresponding to a total integrated luminosity of $\mathcal{L} = 0.94$ fb^{-1}. The main SM process is the electron pair production $ep \to (e)eeX$ where often one electron undetected escapes down the beampipe. Overall, good agreement between the data and the SM expectation is found. At $\sum P_T > 100$ GeV nine events are observed in total, compared to a SM expectation of 5.3 ± 0.6 events. The ex-

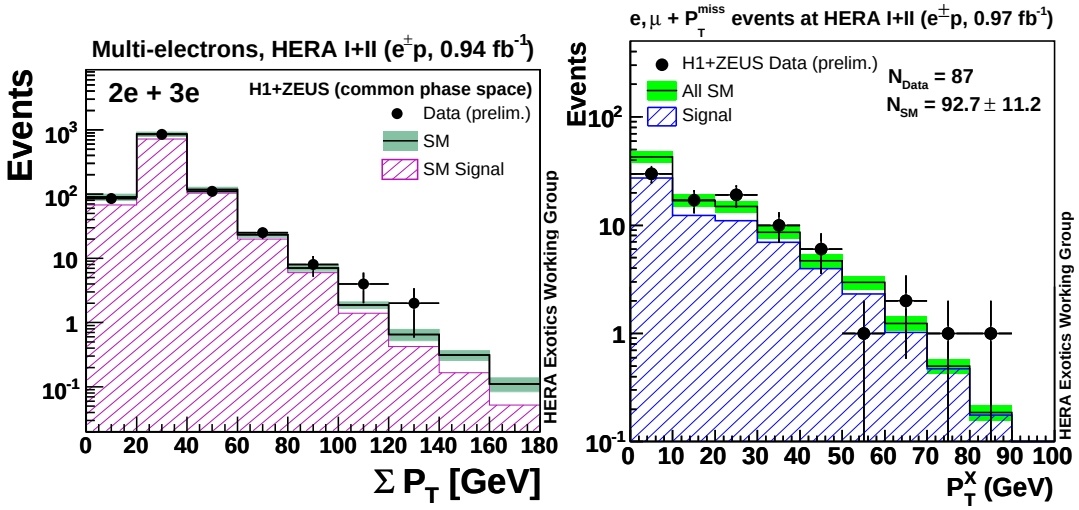

Figure 3: Left: Distribution of the scalar sum of the transverse momenta of the combined 2 and 3 electron events using all HERA I+II data sets from H1 and ZEUS. The data (points) are compared to the SM expectation (open histogram). Right: The hadronic transverse momentum distribution of the combined H1 and ZEUS $e^{\pm}$ data (HERA I+II). The data (points) are compared to the SM expectation (open histogram). The signal component of the SM expectation, dominated by W production, is given by the hatched histogram. N_{Data} is the total number of events observed, N_{SM} is the total SM expectation. Both: The total error on the SM expectations is given by the shaded band.

cess of data at $\sum P_T > 100$ comes from the H1 dataset alone [4] and is not seen in the ZEUS data. Similar analyses containing one or several muons in the final state have been recently published by H1 using the full HERA data set [4]. Also in these channels with muons, which are awaiting combination with ZEUS data, a slight excess in the region $\sum P_T > 100$ is found.

Another interesting final state topology consists of a high P_T lepton and missing transverse momentum. In the SM this topology is mainly due to the production of single W-bosons with subsequent leptonical decay. Combining the HERA I+II data sets from H1 and ZEUS, corresponding to an integrated luminosity of $\mathcal{L} = 0.97$ fb^{-1}, events containing either an electron or a muon are selected. In the common H1/ZEUS phase space in total 87 events are observed corresponding to a SM expectation of 93 ± 11 events. The measured transverse momentum distribution of the hadronic final state P_T^X is shown in Fig. 3 (right) and compared to the SM expectation. Overall good agreement between data and Monte Carlo is found. For $P_T^X > 25$ GeV, a region where an excess was reported by the H1 collaboration [2], 29 events are observed in the common H1/ZEUS phase space in agreement to a SM expectation of 25.3±3.2 events.

The W enriched isolated lepton sample from H1 is also used to measure the W-polarisation by studying the decay angle in the rest frame of the W-boson. Within the large errors good agreement with the SM expectation is found. For more details see [3]. The polarisation amplitudes depend on the production mechanism of the W-boson and are SM-like for ordinary

single W boson production. However, they differ if the W-boson originates for example from a decay of a top quark, which can be anomalously produced at HERA, if the magnetic type coupling $\kappa_{tu\gamma}$ or the vector type coupling v_{tuZ} are different from zero. A more direct way of testing these anomalous couplings is the search for top quark final states. Such a search is performed by H1 and no sign for anomalous top quark production is found, see also [3]. A limit of $\kappa_{tu\gamma} < 0.14$ is set from the H1 data alone, which is the most stringent limit from collider experiments.

4 Proton Structure

The most precise determination of the proton structure is achieved by measuring the inclusive cross section of deep inelastic scattering (DIS). Double differential cross sections were measured by the H1 [5, 6] and ZEUS [7] collaborations using the HERA I data as function of Q^2 and the Bjorken variable x, which describes the fractional momentum of the scattered parton in the naive quark parton model (QPM). Due to the large centre of mass energy a wide kinematic range can be explored by HERA to study the QCD dynamics at small x. Results of a model independent combination of the published H1 and ZEUS measurements based on neutral current (NC) and charged current (CC) data are presented at this workshop [8]. For the combination an averaging procedure is used, which is based on the assumption that H1 and ZEUS experiments measure the same cross section at the same kinematic points. This method takes systematic uncertainties both uncorrelated and correlated for the two experiments into account. The H1-ZEUS combined double differential cross section results have substantially reduced errors compared to the individual experiments and represent the most precise determination of the DIS cross sections at HERA. The combined data also serve as basis for a new precise fit of the proton PDFs, see presentation by [9]. The H1 and ZEUS combined cross sections and the new fit of the proton PDF is shown in Fig. 4.

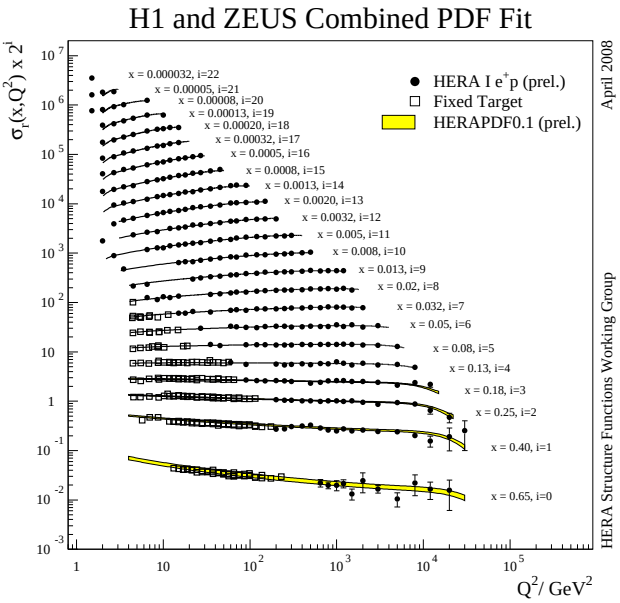

Figure 4: The reduced cross section $\sigma_r(x, Q^2)$ as function of Q^2 for various values of x obtained by combining H1 and ZEUS data from HERA I. Also shown is a new fit of the proton PDFs to the combined data set.

For not too high values of Q^2, where electroweak effects have to be taken into account, the reduced NC cross sections can be written as $\sigma_r = F_2 - \frac{y^2}{Y_+} F_L$, where y is the inelasticity and $Y_+ = 1 + (1 - y)^2$. The structure function F_2, which is dominant except for very large values of y, is related to the charge density of partons in the proton. The structure function

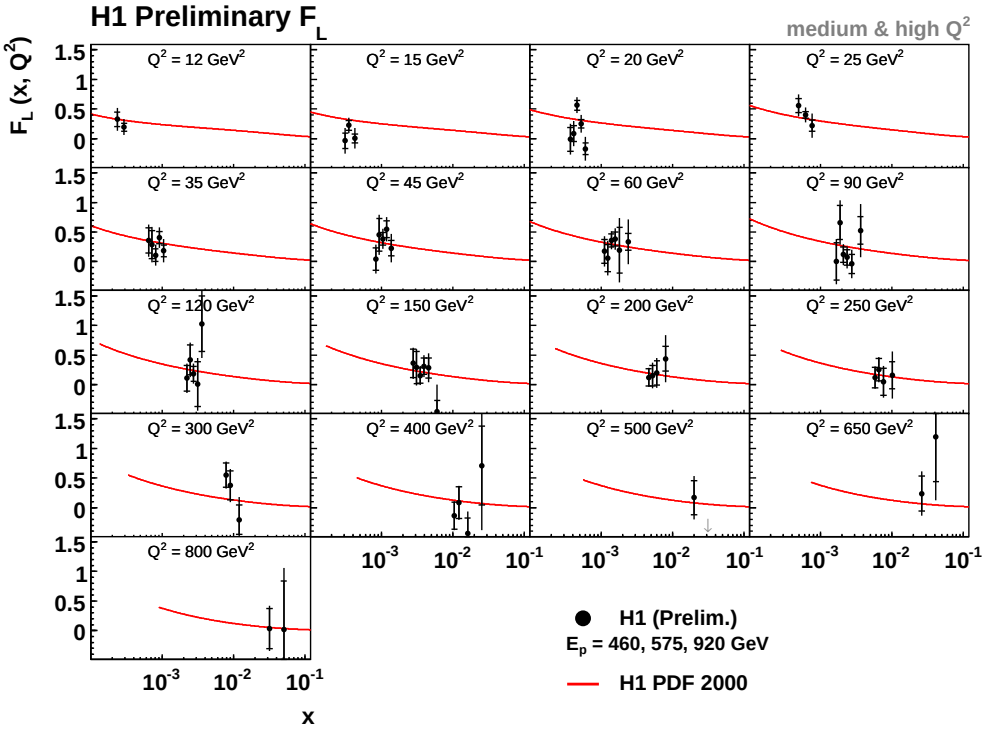

Figure 5: The longitudinal structure function $F_L(x, Q^2)$. The inner error bars denote the statistical error, the full error bars include the systematic error. The luminosity uncertainty is not included in the error bars. The curve represents the NLO QCD prediction derived from the H1 PDF 2000 fit to previous H1 data.

F_L, which can be as large as F_2, corresponds to the cross section of longitudinally polarised virtual photons. The QPM predicts $F_L = 0$. In QCD, however, F_L is non-zero and can be related to the gluon density of the proton. A measurement of F_L can therefore be regarded as a consistency check of perturbative QCD calculations based on the gluon density extracted from scaling violation.

Previous determinations of F_L at HERA [6, 10] were based on extrapolating the structure function F_2 to large values of y (corresponding to small values of x). These indirect determinations were assuming for F_2 a power law function: $F_2 \sim x^{-\lambda(Q^2)}$. At this workshop the first direct measurement of F_L is presented, see for details [11, 12, 13]. The measurement of F_L requires several sets of cross sections at fixed Q^2 and x but at different y. This was achieved by lowering the proton beam energy according to $y = Q^2/(4xE_pE_e)$ whilst keeping the positron beam energy E_e constant. The datasets with lowered proton beam energies of $E_p = 460$ ($E_p = 575$) GeV were taken in dedicated runs from April to June 2008 and correspond to integrated luminosities of $\mathcal{L} = 12.4$ (6.2) pb^{-1}. The big challenge of the F_L measurement is the determination of the cross section at large values of y, which correspond to small scattered positron energies according to $E'_e \sim (1 - y)\, E_e$. The scattered positron is detected either in the SPACAL detector at large polar angles ($\Theta > 155°$) or in the LAr

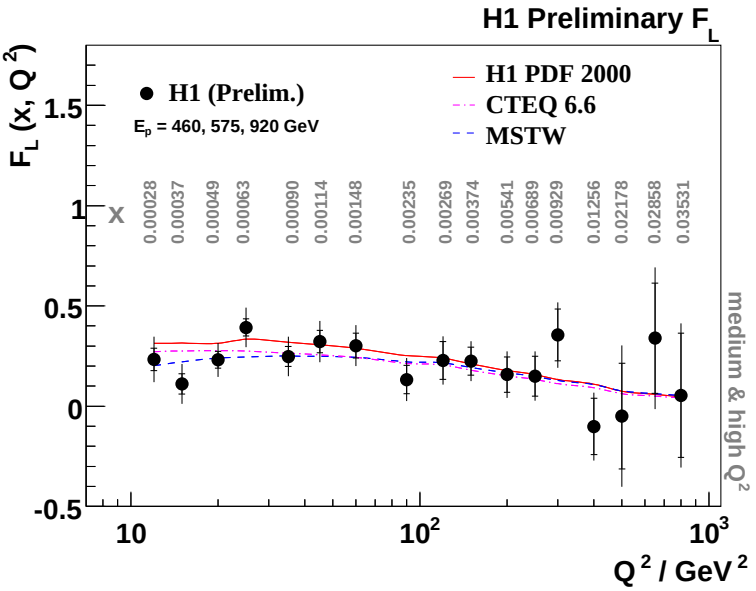

Figure 6: The longitudinal structure function F_L shown as function of Q^2 at the given values of x. The inner error bars denote the statistical error, the full error bars include the systematic errors. The luminosity uncertainty is not included in the error bars. The solid curve describes the expectation on F_L from the H1 PDF 2000 fit using NLO QCD. The dashed (dashed-dotted) curve is the expectation of the MSTW (CTEQ) group using NNLO (NLO) QCD. The theory curves connect predictions at the given (x, Q^2) values by linear extrapolation.

calorimeter ($\Theta < 155°$). For small positron energies the background from photoproduction, where one of the hadronic final state particles is wrongly identified as positron, is large. This background is estimated by using Monte Carlo simulations and data by measuring the charge of the assigned track of the scattered positron candidate, which in photoproduction turns out to be almost equally populated between electron and positron candidates. The estimated photoproduction background is statistically subtracted from the DIS sample. From the y dependence of the cross section for fixed Q^2 and x the structure function F_L is measured. The results are presented in Fig. 5, where F_L is shown as function of x in various bins of Q^2. The results are consistent with the predictions obtained from the H1 PDF 2000 fit [6], which was performed using the high proton energy data from HERA I only.

The values on F_L resulting from averages over x at fixed Q^2 are shown in Fig. 6. The results are compared with QCD predictions based on different parametrisations of the proton PDFs and show good agreement. The results confirm DGLAP QCD predictions for $F_L(x, Q^2)$, determined from previous HERA measurements, which are dominated by a large gluon density at low x. These results present the first measurement of F_L at low x. The results obtained using the SPACAL for positron detection ($Q < 90$ GeV^2) were recently published [14].

5 Exclusive Final States

5.1 Perturbative QCD and Jets

The production of jets at high transverse momentum can be theoretically well described in the framework of perturbative QCD (pQCD) calculations. For HERA only NLO calculations for jet production are available and the largest theoretical uncertainties come from the unknown normalisation and factorization scale reflecting our ignorance about higher order contributions. A pity, as the production of two or more jets in DIS gives direct access to the strong coupling $\alpha_S(M_Z)$, which is one of the fundamental parameters in particle physics. The strong coupling can experimentally be measured at HERA with high precision due to the large statistics of the HERA I+II datasets. The H1 collaboration performed two new measurements of α_S, one in the low Q^2 region, where the scattered electron is detected in the backward SPACAL and one in the high Q^2 region, where the scattered electron is detected in the LAr calorimeter.

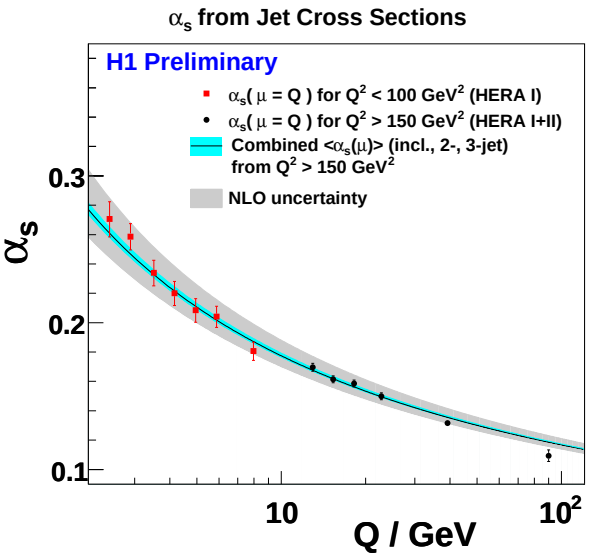

Figure 7: Results of the fitted values of $\alpha_S(\mu = Q)$ from the low Q^2 measurements (red points) and the high Q^2 measurements (black points). The error bars denote the total experimental uncertainty of each data point. The solid curve shows the result of evolving $\alpha_S(M_Z)$ obtained from a fit to the inclusive, dijet and threejet normalised cross section at high Q^2, with the inner blue band denoting the correlated experimental uncertainties and the grey band denoting the theoretical scale uncertainties, PDF uncertainties and the hadronisation corrections.

The measurement at low Q^2 is based on HERA I data only [15]. The kinematic region is defined by $5 < Q^2 < 100$ GeV^2 and $0.2 < y < 0.7$. Jets are selected in the Breit frame using the inclusive k_T algorithm with a minimum transverse momentum of 5 GeV. Inclusive jet cross sections are measured differentially as function of Q^2 and the jet transverse momentum E_T. The measured inclusive cross sections are compared to NLO QCD calculations using the NLOJET++ [16] program. The calculations are performed in the $\overline{\text{MS}}$ scheme for five massive quark flavors and for the PDF parametrisation CTEQ65 [17]. As factorisation scale $\mu_F = Q$ is used, whereas the normalisation scale is chosen to be $\sqrt{(Q^2 + E_T)/4}$. The strong coupling is extracted from the measured distributions and the results are shown as function of the Q in Fig. 7 (red points). A fit to the low Q^2 data yields:

$$\alpha_S(M_Z) = 0.1186 \ \pm \ 0.0014(\text{exp}) \ ^{+0.0132}_{-0.0101}(\text{scale}) \ \pm \ 0.0021(\text{PDF}) \quad , \tag{1}$$

where the first error is due to experimental uncertainties, the second and dominating one from the scale uncertainties and the third from the uncertainty of the PDF.

The measurement of jet rates at high Q^2 is based on HERA I+II data corresponding to a total integrated luminosity of $\mathcal{L} = 395$ pb^{-1} [15]. Jet rates are measured for $160 < Q^2 < 15000$ GeV^2 inclusively, and for 2-jet and 3-jet final states. In contrast to the low Q^2 analysis relative jet rates are measured normalised to the inclusive NC cross section. This reduces the experimental error as the luminosity uncertainty cancels completely and the PDF uncertainties to a large extend. The relative jet rates are measured again as function of Q^2 and E_T in the Breit frame. The strong coupling α_S is extracted in a same way as at low Q^2. The PDFs of the proton are taken from the CTEQ65M set [18]. The extracted α_S values are shown in Fig. 7 as function of Q. A fit to all the high Q^2 jet data yields:

$$\alpha_S(m_Z) = 0.1182 \ \pm \ 0.0008(\text{exp}) \ ^{+0.0041}_{-0.0031}(\text{scale}) \ \pm \ 0.0018(\text{PDF}) \quad , \tag{2}$$

well compatible with the result obtained at low Q^2. This result has a strikingly small experimental error below 1% and is dominated by the large scale uncertainty. The importance of calculating the higher order corrections in order to achieve a precise determination of α_S from the HERA data has to be stressed.

Hard QCD processes are also studied by H1 in prompt photon photoproduction using the full HERA II data. The cross sections are measured in the visible range defined by $5 < E_T^\gamma < 15$ GeV, $Q^2 < 1$ GeV^2, $0.1 < y_h < 0.7$ [a] and $z = E_T^\gamma / E_T^{\text{photon-jet}} > 0.9$. The results, see for more details [19], indicate that the cross sections are in good agreement with QCD NLO calculations [20] and with QCD LO calculations based on k_T factorisation [21] in exclusive final states where a high E_T jet is present. The data, however, overshoot the predictions in the inclusive prompt photon sample for which no jet requirement is applied, see Fig. 8.

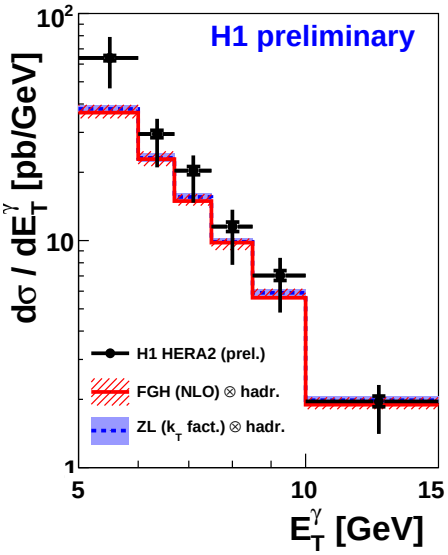

Figure 8: Inclusive prompt photon cross section as function of E_T^γ. The inner error bars represent the statistical errors, while the outer are the statistical and systematical errors added in quadrature. The measured cross section is compared to the Fontannaz-Guillet-Heinrich (continuous red) and the Zotov-Lipatov (dashed blue) calculations.

5.2 Soft QCD and Diffraction

The H1 collaboration has performed a new measurement of the diffractive photoproduction of dijets [23]. They are performed in two different kinematic regions primarily differing in the minimum transverse energy cuts of 5 (7.5) GeV of the two hardest jets. The cross sections are compared with QCD NLO predictions [22], which overshoot the data in both cases. The ratio of the measured cross section over the QCD NLO prediction is shown in Fig. 9 for the case $E_T^{jet1} > 5$ GeV as function of E_T^{jet1}. These new results show a suppression as function

[a] The variable y_h is defined as $y_h = \sum(E - pz)/2E_e$ where the sum is executed over all final state particles.

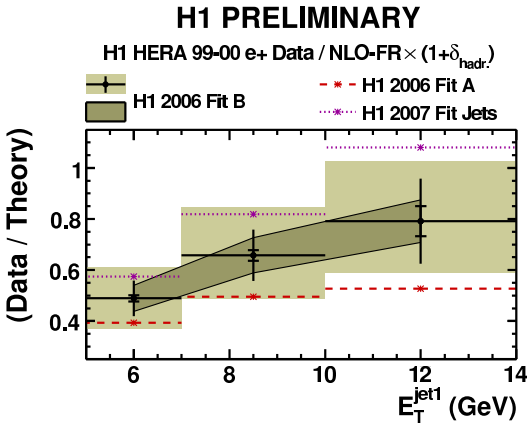

Figure 9: Distribution of the differential cross section $d\sigma/dE_T^{jet1}$ normalised to the NLO-FR calculation based on the H1 2006 Fit B DPDF set and corrected for hadronisation effects. The points show the data, the inner error bars on the points are statistical and the outer error bars show statistical and uncorrelated uncertainties added in quadrature. The correlated systematic errors are indicated by the dark band. The effect on the NLO-FR calculation of varying μ_r by factors of 0.5 and 2.0 is shown in the light band. Also indicated are the central values obtained when the H1 2006 Fit A or H1 2007 Fit Jets DPDFs are used.

of E_T^{jet1} and suggest a suppression factor of about 0.5 at small values of E_T^{jet1}. The suppression is found to have no significant dependence on the photon four-momentum fraction entering the hard subprocess and confirms previous results obtained by the H1 collaboration [24].

5.3 Physics with Flavours

The H1 collaboration reported in [25] evidence for a narrow resonance decaying into a $D^{\pm *}$ meson and a proton at an invariant mass of 3.1 GeV. The charmed meson was identified in the golden decay channel $D^{\pm *} \to K^{\mp}\pi^{\pm}\pi^{\pm}$ and low momentum protons were identified by means of measuring the specific energy loss. This D^*p resonance was not seen by other collider experiments and could also not be confirmed by the ZEUS collaboration. Using the full HERA II statistics this analysis is repeated in a limited phase space region due to the smaller acceptance of the backward SPACAL detector at HERA II. This new sample corresponds to an integrated luminosity of $\mathcal{L} = 348\text{pb}^{-1}$, which is about 5 times the luminosity of the previously analysed HERA I data, where the excess was observed. For the new HERA II data no excess of events in the region of interest is observed, see [26]. An upper limit on the production of such a resonance is set at 1.0 per mille on the ratio of resonant D^*p to D^* production at 95% confidence level using statistical errors only.

New results on the study of D^* production in DIS using the full HERA II dataset are presented on this conference, see also [27]. The data were taken in the years 2004-2007 and correspond to an integrated luminosity of $\mathcal{L} = 347$ pb^{-1}. Single and double differential cross sections are measured in the kinematic range defined by $5 < Q^2 < 100$ GeV^2 and $0.02 < y < 0.7$. The visible range of the D^* mesons is defined by $p_T(D^*) > 1.5$ GeV and

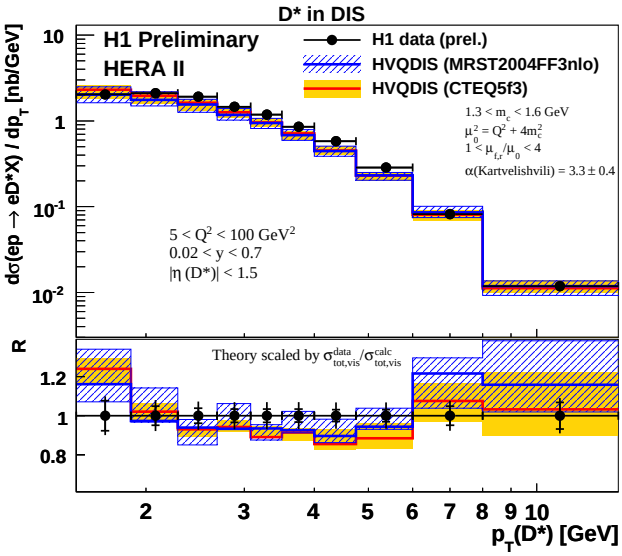

Figure 10: Differential DIS cross section of D^* mesons as a function of $p_T(D^*)$. The measurements are given as black points; the inner error bars correspond to the statistical, the outer to the total systematic error. The bands reflecting the theoretical uncertainties are obtained by varying the charm mass, the scale and the fragmentation parameters. In the lower part the ratio of the normalised differential cross sections data over prediction is shown.

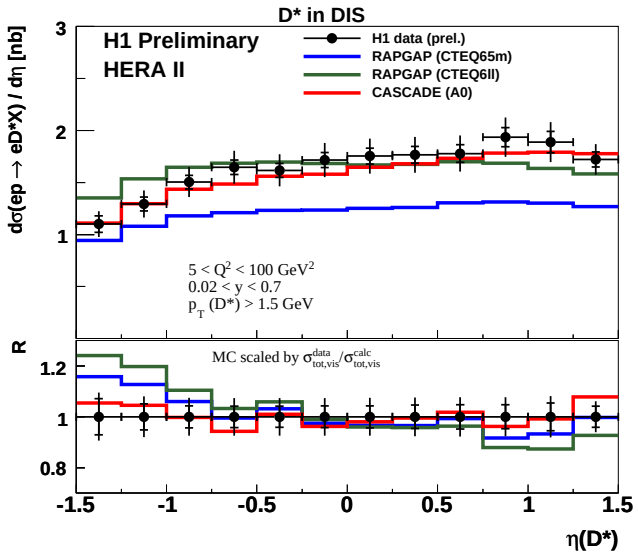

Figure 11: Differential DIS cross section of D^* mesons as a function of the pseudorapidity. For comparison LO Monte Carlo predictions from RAPGAP with PDFs from CTEQ65m (blue histogram) and from CTEQ6ll (green histogram) and from CASCADE with the A0 unintegrated PDF (red histogram) are shown. See also Fig. 10 for explanations.

$|\eta(D^*)| < 1.5$. The results are compared with the LO Monte Carlo programs RAPGAP and CASCADE, and with the NLO program HVQDIS. The distribution of the transverse momentum of the selected D^* mesons $p_T(D^*)$ is shown in Fig. 10 and compared with the NLO predictions from HVQDIS for two different proton PDFs. Within the errors agreement with the NLO calculation and the MRST2004FF3nlo set [28] of the proton densities is found. The data agree not so well with the prediction based on the CTEQ5f3 PDF set [29]. The largest contribution to the uncertainties is of theoretical nature and comes from the scale uncertainty.

The sensitivity to the PDFs is also visible in the pseudorapidity distribution, see Fig. 11, where the measured data points are compared to LO Monte Carlo programs. The best description is found for CASCADE, which is based on unintegrated parton densities. However, it has to be noted that the prediction also depends on the choice of the charm quark mass and the scale parameters.

The production of D^*-mesons can also be studied in the photoproduction regime. A new analysis is presented based on data taken with a dedicated track trigger in the years 2006-2007 corresponding to an integrated luminosity of $\mathcal{L} = 93$ pb^{-1}. D^*-mesons with a minimum transverse momentum of $p_T(D^*) > 1.8$ GeV are selected in the pseudorapidity range $|\eta(D^*)| < 1.5$. Fig. 12 shows the $p_T(D^*)$ distribution of this measurement and the comparison with different LO MC programs. Good agreement of the data with the massless PYTHIA62 prediction is found at low $p_T(D^*)$. At high $p_T(D^*)$ all predictions underestimate the cross section. The shape of the distribution is best described by the CASCADE program, which on the other hand largely underestimates the absolute cross section. More detailed studies are presented in [27], also including comparisons to NLO predictions, which however suffer large scale uncertainties.

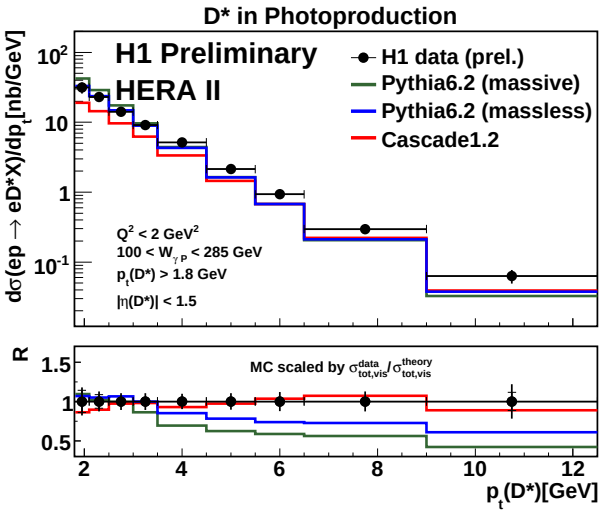

Figure 12: Differential cross section of photoproduced D^* mesons as a function of $p_T(D^*)$. The result is compared to different LO-MC models The green histogram shows the prediction of the PYTHIA62 in the massive scheme, whereas the blue histogram shows the prediction by PYTHIA62 is the massless scheme. The red histogram shows the prediction of CASCADE12. See also Fig. 10 for explanations.

6 Summary

A selection of recent results obtained by the H1 collaboration was presented. The complete list of all new H1 results can be found here [1]. One of the highlights is the first measurement of the structure function F_L at low x, which is based on dedicated datasets taken in 2007

with reduced proton beam energies. These measurements are performed in a large range of Q^2 and are found to be consistent with pQCD predictions.

Many new results like the measurements of the DIS cross sections or the determination of α_S have reached high precision by improving the understanding of the detectors, by exploiting the full HERA datasets and by combination of the H1 and ZEUS data. The HERA experiments are entering the era of high precision measurements with full HERA statistics. Many more exciting results are expected to come in the near future.

References

[1] Slides:
`http://indico.cern.ch/contributionDisplay.py?contribId=1&sessionId=1&confId=24657`

[2] V. Andreev *et al.* [H1 Collaboration], Phys. Lett. B **561** (2003) 241 [hep-ex/0301030].

[3] talk given by E. Rizvi, these proceedings.

[4] F. D. Aaron *et al.* [H1 Collaboration], submitted to Phys. Lett. B, DESY-08/65, [hep-ex/08063987].

[5] C. Adloff *et al.* [H1 Collaboration], Eur. Phys. J. C **13** (2000) 609 [hep-ex/9908059];
ibid., Eur. Phys. J. C 19 (2001) 269 [hep-ex/0012052].

[6] C. Adloff *et al.* [H1 Collaboration], Eur. Phys. J. C **21** (2001) 33 [hep-ex/0012053]; ibid., Eur. Phys. J. C 30 (2003) 1 [hep-ex/0304003].

[7] J. Breitweg *et al.* [ZEUS Collaboration], Eur. Phys. J. C **12** (2000) 411 [Erratum-ibid. C **27** (2003) 305] [hep-ex/9907010];
S. Chekanov *et al.* [ZEUS Collaboration], Eur. Phys. J. C **21** (2001) 443 [hep-ex/0105090];
ibid., Eur. Phys. J. C **28** (2003) 175 [hep-ex/0208040];
ibid., Phys. Lett. B **539** (2002) 197 [Erratum-ibid. B **552** (2003) 308] [hep-ex/0205091];
ibid., Phys. Rev. D **70** (2004) 052001 [hep-ex/0401003];
ibid., Eur. Phys. J. C **32** (2003) 1 [hep-ex/0307043].

[8] talk given by F. Feltesse, these proceedings.

[9] talk given by A.M. Cooper-Sarkar, these proceedings.

[10] C. Adloff *et al.* [H1 Collaboration], Phys. Lett. B **393** (1997) 452 [hep-ex/9611017].

[11] talk given by B. Antonuvic, these proceedings.

[12] talk given by V. Shekelian, these proceedings.

[13] talk given by R. Kogler, these proceedings.

[14] F. D. Aaron *et al.* [H1 Collaboration], Phys. Lett. B **665** (2008) 139 [ep-ex/0805.2809].

[15] talk given by M. Gouzevitch, these proceedings.

[16] Z. Nagy, Z. Trocsanyi, Phys. Rev. Lett. **87** 082001 (2001) [hep-ph/0104315].

[17] D. Stump *et al.*, JHEP 0310 (2003) 46.

[18] J. Pumplin *et al.*, JHEP 0207 (2002) 12 [hep-ph/0201195].

[19] talk given by K. Nowak, these proceedings.

[20] M. Fontannaz, J. P. Guillet and G. Heinrich, Eur. Phys. J. C **21** (2001) 303 [hep-ph/0105121];
M. Fontannaz and G. Heinrich, Eur. Phys. J. C **34**, 191 (2004) [hep-ph/0312009].

[21] A. V. Lipatov and N. P. Zotov, Phys. Rev. D **72** (2005) 054002 [hep-ph/0506044].

[22] S. Frixione, Z. Kunzst and A. Signer, Nucl. Phys. B **467** (1996) 399 [hep-ph/9512328];
S. Frixione, Nucl. Phys. B **507** (1997) 295 [hep-ph/9706545].

[23] talk given by K. Cerny, these proceedings.

[24] A. Aktas *et al.* [H1 Collaboration], Eur. Phys. J. C **51** (2007) 549.

[25] A. Aktas *et al.* [H1 Collaboration], Phys. Lett. B **588** (2004) 17 [hep-ex/0403017].

[26] talk given by K. Krüger, these proceedings.

[27] talk given by A. Jung, these proceedings.

[28] A. D. Martin, W. J. Stirling and R. S. Thorne, Phys. Lett. B **636** (2006) 259 [hep-ph/0603142].

[29] H. L. Lai *et al.*, Eur. Phys. J C **12** (2000) 375 [hep-ph/9903282].